Stability Analysis of Shells Using a NURBS-based Isogeometric Approach

Matheus Pascoal Martins de Sousa[1], John Williams Ferreira de Souza[1], Elias Saraiva Barroso[1], Evandro Parente Jr.[1], João Batista Marques de Sousa Junior[1].

[1]*Laboratório de Mecânica Computacional e Visualização (LMCV), Departamento de Engenharia Estrutural e Construção Civil, Universidade Federal do Ceará, Campus do Pici, Bloco 728, 60440-900, Fortaleza/CE-Brazil*
matheuspmsousa@alu.ufc.br, johnwilliams@alu.ufc.br, elias.barroso@ufc.br, evandro@ufc.br, joaobatistasousajr@ufc.br

Abstract. Shells are structures sensitive to buckling due to their characteristic high slenderness. Thus, the evaluation of buckling loads and the study of the post-buckling behavior are essential. Isogeometric analysis has been widely used in analysis of shells, due to its ability to accurately represent the geometry of the structure regardless of the discretization level and the simplicity of model refinement procedures. The aim of this work is to evaluate the stability of shells through an isogeometric approach, considering large displacements and moderate rotations. This formulation is based on the Reissner-Mindlin theory for thick shells and the degenerated continuum approach using NURBS as basis functions. The proposed formulation is applied in the stability analysis of plates and shells, where critical loads and equilibrium paths are evaluated and compared to solutions available in the literature or obtained by the Finite Element Method.

Keywords: Shells, Stability, Isogeometric Analysis, NURBS

1 Introduction

Shells are curved surface structures whose thickness is much smaller than other dimensions. They are present in several areas of engineering, being widely used in civil, aeronautical, mechanical, automotive, and naval structures. These structures are subject to collapse triggered by the loss of stability due to their characteristic high slenderness. Thus, nonlinear analyzes are necessary, in which the consideration of large displacements is essential.

There are numerous analysis methods that can be used to model these problems, with Finite Element Method (FEM) being currently the most used. However, due to the imperfections sensitivity presented in the mechanical behavior of shells, Isogeometric Analysis (IGA) has become relevant due to its ability to accurately represent the geometry of the problem regardless of the level of discretization considered, eliminating the error in the representation of the geometry that exists in FEM. Additionally, the B-Splines and NURBS have a greater degree of continuity than those normally used in FEM, which can make IGA have a faster convergence than FEM.

Research involving isogeometric analysis of shells are reported in the literature after the proposal of IGA concept [1], where several formulations of isogeometric shells have been discussed in the context of linear and nonlinear analyses. Formulations based in Kirchhoff-Love theory are developed in context of IGA, where analysis models with C^1 bases are easily obtainable, as in NURBS-based models [2]. Likewise, Reissner-Mindlin transverse shear formulations are also studied. In this context, a formulation based on the degenerated solid approach was initially proposed by Uhm and Youn [3] for T-Splines, which was later extended to a nonlinear formulation for isogeometric analysis by Dornisch et al. [4], using precisely calculated director vectors for NURBS. Recent research on isogeometric buckling analysis of complex shells with variable stiffness was done by Hao et al. [5].

In this work, a nonlinear NURBS-based isogeometric formulation is presented for the stability analysis of shells, using the Reissner-Mindlin theory and the degenerated solid approach.

The rest of the paper is organized as follows. Section 2 introduces the degenerated solid approach. Section 3 describes the nonlinear isogeometric formulation. Section 4 presents some numerical examples used to assess the efficiency of the present formulation. Finally, Section 5 expresses the concluding remarks of the study.

2 Degenerated Solid Approach for Analysis of Shells

In the degenerated solid approach, the geometry of the shell is represented a point $\mathbf{x}$ of the mid-surface, by the unit normal vector $\mathbf{v}_3$ and the thickness t in $\mathbf{x}$. Thus, a point $\overline{\mathbf{x}}$ within the shell is defined by:

$$\overline{\mathbf{x}}(\xi,\eta,\zeta) = \mathbf{x}(\xi,\eta) + \zeta\,\frac{t(\xi,\eta)}{2}\,\mathbf{v}_3(\xi,\eta), \tag{1}$$

where $\mathbf{v}_3 = (l_3,\, m_3,\, n_3)^T$, $-1 \le \xi \le +1$, $-1 \le \eta \le +1$ are the parametric coordinates tangent to the shell surface, and $-1 \le \zeta \le +1$ is the parametric coordinate along the thickness.

In this work, a Total Lagrangian formulation [6] is used, which considers large displacements and moderate rotations, but small strains. Stresses and strains are always evaluated in the initial configuration of the structure.

The displacements inside the model are given by:

$$\overline{\mathbf{u}}(\xi,\eta,\zeta) = \mathbf{u}(\xi,\eta) + \zeta\,\frac{t(\xi,\eta)}{2}\left(-\alpha\,\mathbf{v}_2(\xi,\eta) + \beta\,\mathbf{v}_1(\xi,\eta)\right), \tag{2}$$

where $\mathbf{v}_1 = (l_1,\, m_1,\, n_1)^T$ and $\mathbf{v}_2 = (l_2,\, m_2,\, n_2)^T$ are unit tangent director vectors, α and β are the rotations of the normal vector in relation to axes $\mathbf{v}_1$ and $\mathbf{v}_2$. The director vectors $\mathbf{v}_1$, $\mathbf{v}_2$ and $\mathbf{v}_3$ are perpendicular to each other. The Green-Lagrange strains, which have a linear term $\boldsymbol{\varepsilon}_0$ and a quadratic term $\boldsymbol{\varepsilon}_L$, within the shell are computed from the displacement derivatives with respect to the Cartesian coordinates:

$$\boldsymbol{\varepsilon} = \begin{Bmatrix} \varepsilon_x \\ \varepsilon_y \\ \varepsilon_z \\ \gamma_{xy} \\ \gamma_{xz} \\ \gamma_{yz} \end{Bmatrix} = \begin{Bmatrix} \overline{u}_{,x} \\ \overline{v}_{,y} \\ \overline{w}_{,z} \\ \overline{u}_{,y} + \overline{v}_{,x} \\ \overline{w}_{,x} + \overline{u}_{,z} \\ \overline{v}_{,z} + \overline{w}_{,y} \end{Bmatrix} + \frac{1}{2}\begin{Bmatrix} \overline{u}_{,x}^2 + \overline{v}_{,x}^2 + \overline{w}_{,x}^2 \\ \overline{u}_{,y}^2 + \overline{v}_{,y}^2 + \overline{w}_{,y}^2 \\ \overline{u}_{,z}^2 + \overline{v}_{,z}^2 + \overline{w}_{,z}^2 \\ 2(\overline{u}_{,x}\,\overline{u}_{,y} + \overline{v}_{,x}\,\overline{v}_{,y} + \overline{w}_{,x}\,\overline{w}_{,y}) \\ 2(\overline{u}_{,x}\,\overline{u}_{,z} + \overline{v}_{,x}\,\overline{v}_{,z} + \overline{w}_{,x}\,\overline{w}_{,z}) \\ 2(\overline{u}_{,y}\,\overline{u}_{,z} + \overline{v}_{,y}\,\overline{v}_{,z} + \overline{w}_{,y}\,\overline{w}_{,z}) \end{Bmatrix} = \boldsymbol{\varepsilon}_0 + \boldsymbol{\varepsilon}_L. \tag{3}$$

The relationship between the Piola-Kirchhoff II stresses and the Green-Lagrange strains in the local system is given by the generalized Hooke's law [7]:

$$\boldsymbol{\sigma}' = \mathbf{C}'\,\boldsymbol{\varepsilon}'. \tag{4}$$

The local system (x', y', z'), where the material properties of the shell are defined, is given by the director vectors $\mathbf{v}_1$, $\mathbf{v}_2$, and $\mathbf{v}_3$. The material properties are transformed to the global system of the problem, where the strain-displacement matrix is defined and the equilibrium of the structure is established. Strains in global system ($\boldsymbol{\varepsilon}$) are related to local strains ($\boldsymbol{\varepsilon}'$) using the transformation matrix $\mathbf{T}$ [7]:

$$\boldsymbol{\varepsilon}' = \mathbf{T}\,\boldsymbol{\varepsilon}. \tag{5}$$

Moreover, the stresses and the constitutive matrix can be obtained in the global system in the same manner:

$$\boldsymbol{\sigma} = \mathbf{T}^T\,\boldsymbol{\sigma}' \quad \Rightarrow \quad \boldsymbol{\sigma} = \mathbf{C}\,\boldsymbol{\varepsilon} \quad \Rightarrow \quad \mathbf{C} = \mathbf{T}^T\,\mathbf{C}'\,\mathbf{T}. \tag{6}$$

3 Isogeometric Formulation

A NURBS surface is defined by a given control net $\mathbf{P}_a(n \times m)$, and knot vectors $\Xi = [\xi_1, \xi_2, ..., \xi_{n+p+1}]$ and $\Omega = [\eta_1, \eta_2, \ldots, \eta_{n+p+1}]$ as:

$$S(\xi,\eta) = \sum_{a=1}^{np} R_a(\xi,\eta)\,\mathbf{P}_a. \tag{7}$$

where np is the number of control points and $R_a(\xi,\eta)$ are the bivariate rational basis functions given by:

$$R_a(\xi,\eta) = \frac{N_{i,p}(\xi)\,N_{j,q}(\eta)\,w_{ij}}{\sum_{\hat{i}=1}^{n}\sum_{\hat{j}=1}^{m} N_{\hat{i},p}(\xi)\,N_{\hat{j},q}(\eta)\,w_{\hat{i}\hat{j}}} = \frac{N_{i,p}(\xi)\,N_{j,q}(\eta)\,w_{ij}}{W(\xi,\eta)}, \tag{8}$$

where $N_{i,p}(\xi)$ and $N_{j,q}(\eta)$ are univariate B-Splines basis functions, w_{ij} is the control point weight, and $W(\xi,\eta)$ is the bivariate weighting function. It is worth noting that the global basis index a is related to tensor product basis indexes (i,j) by:

$$a = m(i-1)+j, \qquad i=1,2,\dots n, \qquad j=1,2,\dots m \quad \text{and} \quad np = m\,n. \tag{9}$$

Using the degenerated solid approach, the shell mid-surface $(\mathbf{x})$, normal vector $(\mathbf{v}_3)$, and thickness (t) are defined as:

$$\mathbf{x} = \sum_{a=1}^{np} R_a\,\mathbf{x}_a, \qquad \mathbf{v}_3 = \sum_{a=1}^{np} R_a\,\mathbf{v}_{3a}, \qquad t = \sum_{a=1}^{np} R_a\,t_a, \tag{10}$$

where $\mathbf{x}_a$ are the shell control points, $\mathbf{v}_{3a}$ is a normalized director vector, and t_a the thickness associated with control point a. Substituting Eq. (10) in Eq. (1), the geometry of the NURBS shell element is written as:

$$\begin{Bmatrix} x \\ y \\ z \end{Bmatrix} = \sum_{a=1}^{np} R_a \begin{Bmatrix} x_a \\ y_a \\ z_a \end{Bmatrix} + \sum_{a=1}^{np} R_a\,\zeta\frac{t_a}{2}\begin{Bmatrix} l_{3a} \\ m_{3a} \\ n_{3a} \end{Bmatrix}. \tag{11}$$

According to the isogeometric approach, the same basis functions used to describe the geometry are used to approximate the displacement field within the shell:

$$\begin{Bmatrix} u \\ v \\ w \end{Bmatrix} = \sum_{a=1}^{np} R_a \begin{Bmatrix} u_a \\ v_a \\ w_a \end{Bmatrix} + \sum_{a=1}^{np} R_a\,\zeta\frac{t_a}{2}\begin{Bmatrix} \beta_a\,l_{1a} - \alpha_a\,l_{2a} \\ \beta_a\,m_{1a} - \alpha_a\,m_{2a} \\ \beta_a\,n_{1a} - \alpha_a\,n_{2a} \end{Bmatrix}, \tag{12}$$

where α_a and β_a are independent rotations, around local axes $\mathbf{v}_{1a}$ and $\mathbf{v}_{2a}$, associated with control points a and perpendicular to each other and to $\mathbf{v}_{3a}$. The displacement field can be written in matrix form as:

$$\bar{\mathbf{u}} = \begin{bmatrix} u \\ v \\ w \end{bmatrix} = \sum_{a=1}^{np} \begin{bmatrix} R_a & 0 & 0 & g_{11}\,H_a & g_{21}\,H_a \\ 0 & R_a & 0 & g_{12}\,H_a & g_{22}\,H_a \\ 0 & 0 & R_a & g_{13}\,H_a & g_{23}\,H_a \end{bmatrix} \begin{bmatrix} u_a \\ v_a \\ w_a \\ \alpha_a \\ \beta_a \end{bmatrix} = \sum_{a=1}^{np} \mathbf{N}_a\,\mathbf{u}_a = \mathbf{N}\,\mathbf{u}, \tag{13}$$

where

$$H_a = R_a\,\zeta, \tag{14}$$

$$g_{11} = -\frac{1}{2}t_a\,l_{2a}, \qquad g_{12} = -\frac{1}{2}t_a\,m_{2a}, \qquad g_{13} = -\frac{1}{2}t_a\,n_{2a}, \tag{15}$$

$$g_{21} = \frac{1}{2}t_a\,l_{1a}, \qquad g_{22} = \frac{1}{2}t_a\,m_{1a} \quad \text{and} \quad g_{23} = \frac{1}{2}t_a\,n_{1a}. \tag{16}$$

Using Eqs. (3), (12), and (13), the relation between the strain vector within the shell $(\boldsymbol{\varepsilon})$ and the vector of degrees of freedom $(\mathbf{u})$ can be written as:

$$\boldsymbol{\varepsilon} = \boldsymbol{\varepsilon}_0 + \boldsymbol{\varepsilon}_L = \mathbf{H}\,\boldsymbol{\beta} + \frac{1}{2}\,\mathbf{A}\,\boldsymbol{\beta} = \mathbf{H}\,\mathbf{G}\,\mathbf{u} + \frac{1}{2}\mathbf{A}\,\mathbf{G}\,\mathbf{u} = \left(\mathbf{B}_0 + \frac{1}{2}\mathbf{B}_L\right)\,\mathbf{u} = \mathbf{B}\,\mathbf{u}, \tag{17}$$

where

$$\boldsymbol{\beta} = \begin{Bmatrix} u_{,x} \\ u_{,y} \\ u_{,z} \\ v_{,x} \\ \vdots \\ w_{,z} \end{Bmatrix} = \sum_{a=1}^{np} \begin{bmatrix} R_{a,x} & 0 & 0 & g_{11}\,H_{a,x} & g_{21}\,H_{a,x} \\ R_{a,y} & 0 & 0 & g_{11}\,H_{a,y} & g_{21}\,H_{a,y} \\ R_{a,z} & 0 & 0 & g_{11}\,H_{a,z} & g_{21}\,H_{a,z} \\ 0 & R_{a,x} & 0 & g_{12}\,H_{a,x} & g_{22}\,H_{a,x} \\ \vdots & \vdots & \vdots & \vdots & \vdots \\ 0 & 0 & R_{a,z} & g_{13}\,H_{a,z} & g_{23}\,H_{a,z} \end{bmatrix} \begin{bmatrix} u_a \\ v_a \\ w_a \\ \alpha_a \\ \beta_a \end{bmatrix} = \sum_{a=1}^{np} \mathbf{G}_a\,\mathbf{u}_a = \mathbf{G}\,\mathbf{u}, \tag{18}$$

with

$$H_{a,x} = R_{a,x}\,\zeta + R_a\,\zeta_{,x}, \qquad H_{a,y} = R_{a,y}\,\zeta + R_a\,\zeta_{,y} \quad \text{and} \quad H_{a,z} = R_{a,z}\,\zeta + R_a\,\zeta_{,z}. \tag{19}$$

Due to the use of the degenerated solid approach, matrices $\mathbf{H}$ and $\mathbf{A}$ are the same ones of 3D continuum elements [8].

According to Eqs. (17), (18) and (19), matrices $\mathbf{G}$, $\mathbf{B}_0$ and $\mathbf{B}_L$ depend on the the derivatives of the basis functions R_a and ζ function with respect to the Cartesian coordinates (x, y, z). However, these functions are defined in terms of parametric coordinates (ξ, η, ζ). In this work, the ζ coordinate is handled as an additional shape function and the required derivatives with respect to the Cartesian coordinates are computed from:

$$\begin{bmatrix} R_{a,x} \\ R_{a,y} \\ R_{a,z} \end{bmatrix} = \mathbf{J}^{-1} \begin{bmatrix} R_{a,\xi} \\ R_{a,\eta} \\ 0 \end{bmatrix} \quad \text{and} \quad \begin{bmatrix} \zeta_{,x} \\ \zeta_{,y} \\ \zeta_{,z} \end{bmatrix} = \mathbf{J}^{-1} \begin{bmatrix} 0 \\ 0 \\ 1 \end{bmatrix}, \tag{20}$$

where the Jacobian matrix ($\mathbf{J}$) is given by:

$$\mathbf{J} = \begin{bmatrix} \sum R_{a,\xi} \left(x_a + \zeta \frac{t_a}{2} l_{3a} \right) & \sum R_{a,\xi} \left(y_a + \zeta \frac{t_a}{2} m_{3a} \right) & \sum R_{a,\xi} \left(z_a + \zeta \frac{t_a}{2} n_{3a} \right) \\ \sum R_{a,\eta} \left(x_a + \zeta \frac{t_a}{2} l_{3a} \right) & \sum R_{a,\eta} \left(y_a + \zeta \frac{t_a}{2} m_{3a} \right) & \sum R_{a,\eta} \left(z_a + \zeta \frac{t_a}{2} n_{3a} \right) \\ \sum R_a \frac{t_a}{2} l_{3a} & \sum R_a \frac{t_a}{2} m_{3a} & \sum R_a \frac{t_a}{2} n_{3a} \end{bmatrix}. \tag{21}$$

3.1 Equilibrium equations

The static equilibrium equations of the model can be obtained using the Principle of Virtual Work:

$$\delta U = \delta W_{ext} \Rightarrow \int_V \delta\boldsymbol{\varepsilon}^T \boldsymbol{\sigma}\, dV = \int_V \delta\mathbf{u}^T \mathbf{b}\, dV + \int_S \delta\mathbf{u}^T \mathbf{q}\, dS, \tag{22}$$

where $\delta\mathbf{u}$ is the virtual displacement vector, $\delta\boldsymbol{\varepsilon}$ is the virtual strain vector, and $\mathbf{q}$ and $\mathbf{b}$ are the surface and body loads, respectively. This equation can be rewritten to include a residue $\mathbf{r}$ which represents the imbalance between internal ($\mathbf{g}$) and external forces ($\mathbf{f}$), and so, for displacement-independent loads, the nonlinear equilibrium can be written as:

$$\mathbf{r}(\mathbf{u}, \lambda) = \mathbf{g}(\mathbf{u}) - \lambda \mathbf{f}, \tag{23}$$

where:

$$\mathbf{g} = \int_V \overline{\mathbf{B}}^T \boldsymbol{\sigma}\, dV, \qquad \mathbf{f} = \int_V \mathbf{N}^T \mathbf{b}\, dV + \int_S \mathbf{N}^T \mathbf{q}\, dS, \tag{24}$$

and λ is the load factor. The equation is solved in each step for $\mathbf{r} = 0$ using an appropriate path-following method, such as the Load Control, Displacements Control, or the Arc-Length Method, which are based on Newton-Raphson method iterations [8].

The stiffness matrix is obtained by the differentiation of the internal forces vector:

$$\mathbf{K}_T = \frac{\partial \mathbf{g}}{\partial \mathbf{u}} = \mathbf{K}_E + \mathbf{K}_G, \tag{25}$$

where the material stiffness matrix $\mathbf{K}_E$ and the geometric stiffness matrix $\mathbf{K}_G$ are given by:

$$\mathbf{K}_E = \int_V \overline{\mathbf{B}}^T \mathbf{C}\, \overline{\mathbf{B}}\, dV, \qquad \mathbf{K}_G = \int_V \mathbf{G}^T \mathbf{S}\, \mathbf{G}\, dV, \tag{26}$$

where:

$$\overline{\mathbf{B}} = \mathbf{B}_0 + \mathbf{B}_L, \quad \mathbf{S} = \begin{bmatrix} \overline{\mathbf{S}} & \overline{\mathbf{0}} & \overline{\mathbf{0}} \\ \overline{\mathbf{0}} & \overline{\mathbf{S}} & \overline{\mathbf{0}} \\ \overline{\mathbf{0}} & \overline{\mathbf{0}} & \overline{\mathbf{S}} \end{bmatrix}, \quad \overline{\mathbf{0}} = \begin{bmatrix} 0 & 0 & 0 \\ 0 & 0 & 0 \\ 0 & 0 & 0 \end{bmatrix}, \quad \overline{\mathbf{S}} = \begin{bmatrix} \sigma_{xx} & \tau_{xy} & \tau_{xz} \\ \tau_{xy} & \sigma_{yy} & \tau_{yz} \\ \tau_{xz} & \tau_{yz} & \sigma_{zz} \end{bmatrix}. \tag{27}$$

For a more efficient implementation, instead of computing the integrals in the entire volume, we perform the Gaussian integration in the isogeometric element, defined by the knot spans in the parametric directions on the shell surface. This is similar to what is performed in FEM for the assembly of the global stiffness matrix.

The presented isogeometric formulation was implemented in the open-source structural analysis software FAST (Finite Element Analysis Tool), developed in C++ programming language and using the object-oriented programming (OOP) paradigm.

4 Numerical Examples

This section presents the results obtained using the presented isogeometric formulation for stability analysis of shells. These results are compared with analytical and finite element solutions to validate the formulation and its computer implementation. The effect of the numerical integration scheme is also assessed.

In degenerated shell approaches, director vectors are defined at node positions of the FEM model using the geometry model. However, in NURBS-based approach, control points do not interpolate the geometry. Hence, it is necessary to evaluate the corresponding directors at control points that define a suitable normal vector field on the mid-surface of the shell (see Eq. (10)). Here, the normal vectors are obtained by linear regression of the normal vectors computed at ($m \times n$) samples points distributed uniformly over NURBS domain.

4.1 Example 1 - Buckling of a square plate under axial compression

This example deals with the buckling of a simply supported square plate. The plate is subjected to a compressive load (N_x) uniformly distributed along the edge $x = L$. Figure 1a presents the material properties, geometric data, boundary conditions, and loading.

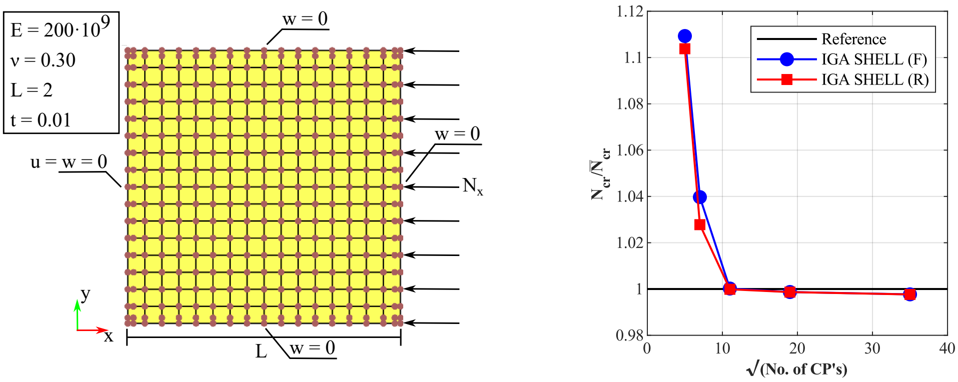

(a) Problem definition and 16 × 16 cubic mesh.

(b) Critical load $\overline{N}_{cr}$ convergence.

Figure 1. Buckling of a square plate.

Figure 1b presents the buckling loads computed for different cubic NURBS meshes using full (F) and reduced (R) integration schemes. The reference buckling load ($\overline{N}_{cr}$) was computed using the classical solution for thin plates [9]. The results show that the proposed formulation converges to values slightly lower (0.23%) than the reference value, due to the use of the Reissner-Mindlin theory. The reduced integration scheme presents a better accuracy, especially for coarse discretizations. However, both integration schemes converge to same same solution under mesh refinement.

4.2 Example 2 - Buckling of a cylindrical shell under axial compression

This example considers the buckling of a simply supported cylindrical shell under axial compression (N_x). Figure 2a presents the material properties, geometric data, boundary conditions, and loading. Figure 2b presents the buckling loads computed for different cubic NURBS meshes using the same two integration schemes. The reference buckling load ($\overline{N}_{cr}$) was computed using the classical solution derived using the Donnell theory [9].

The results show that the proposed formulation converges to values considerably lower (7.14%) than the reference value. This occurs because the classical solution considers a constant pre-buckling distribution of membrane forces, which cannot be obtained using the simply supported boundary conditions. For this reason, Figure 2b also presents the results obtained using FEM and the same boundary conditions. We can see that both IGA and FEM converged to almost identical results. Finally, the results show that the reduced integration alleviates the locking problem, leading to a faster convergence.

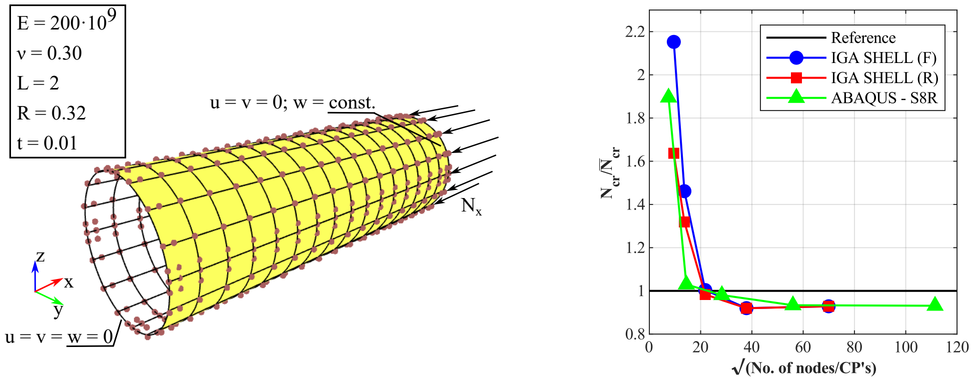

(a) Problem definition and 16 × 16 cubic mesh. (b) Critical load $\overline{N}_{cr}$ convergence.

Figure 2. Buckling of a cylindrical shell.

4.3 Example 3 - Cylindrical panel under point load

This example deal with the nonlinear analysis of a hinged cylindrical panel subjected to a point load at the center, as shown in Figure 3(a). This figure also presents the material properties, geometric data and boundary conditions. Two different thicknesses are considered. Owing to symmetry, only one-quarter of the panel is discretized using cubic NURBS meshes. Only the reduced integration scheme was used in this example. This shell have been analyzed by several authors [10], and is particularly popular due to the snapping behavior.

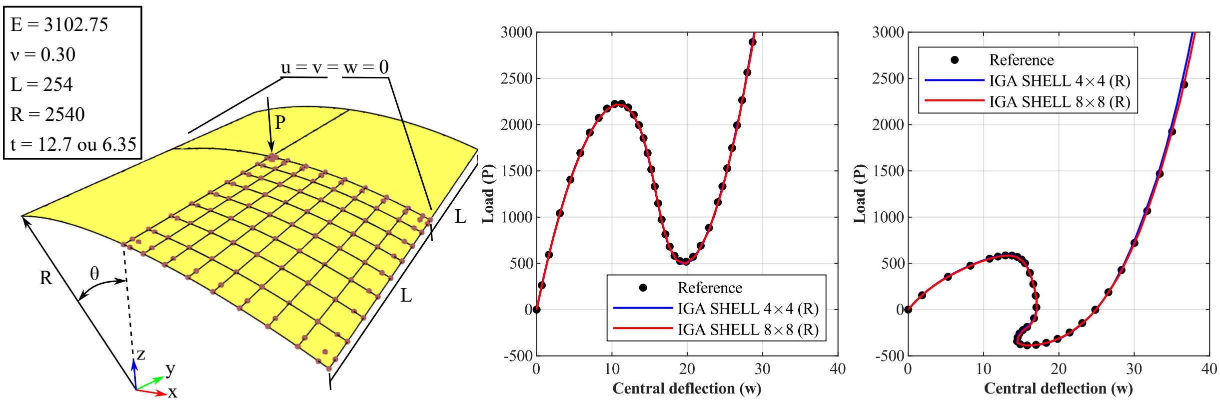

(a) Problem definition and 8 × 8 cubic mesh. (b) Load-deflection for $t = 12.7$. (c) Load-deflection for $t = 6.35$.

Figure 3. Nonlinear analysis of a hinged semi-cylindrical roof.

Figure 3(b) shows the load-displacement curve of the 12.7 thick shell. Accurate results were obtained using a 4×4 cubic NURBS mesh in comparison with the reference results [10]. The curve for the finer mesh (8×8) is almost identical. This shell presents a simple nonlinear behavior, characterized by the presence of limit points and snap-through.

Figure 3(c) shows the results for the 6.35 thick shell. This structure presents a more complex nonlinear behavior, with snap-through and snap-back. Reasonably accurate predictions were obtained using a 4×4 cubic NURBS mesh. The curve for the finer mesh (8×8) is almost identical, but closer to the reference results [10] for larger displacements.

5 Conclusion

This work presented a NURBS-based isogeometric formulation to stability analysis of shells. The formulation was successfully applied to determination of critical loads and nonlinear equilibrium paths. It was observed that, using the reduced integration scheme, the locking phenomenon is alleviated, improving the accuracy of the results and the computational efficiency. However, both integration schemes converged to the same solutions with model refinement.

With the first two examples we were able to test the ability of the formulation to obtain excellent results for buckling loads. Regarding the nonlinear analysis, we saw that the presented formulation was able to trace the equilibrium paths with great accuracy even with coarser meshes. Despite being based on a formulation for considering only moderate rotations, the element was able to represent the nonlinear behavior for considerable displacement values, improving the results with mesh refinement.

Further research will be carried out on the behavior of the proposed formulation on the post-buckling analysis and imperfection sensitivity of shells.

Acknowledgements. The authors gratefully acknowledge the financial support provide by CNPq (Conselho Nacional de Desenvolvimento Científico e Tecnológico) and FUNCAP (Fundação Cearense de Apoio ao Desenvolvimento Científico e Tecnológico).

Authorship statement. The authors hereby confirm that they are the sole liable persons responsible for the authorship of this work, and that all material that has been herein included as part of the present paper is either the property (and authorship) of the authors, or has the permission of the owners to be included here.

References

[1] J. A. Cottrell, T. J. Hughes, and Y. Bazilevs. *Isogeometric analysis: toward integration of CAD and FEA*. John Wiley & Sons, 2009.

[2] J. Kiendl, K.-U. Bletzinger, J. Linhard, and R. Wüchner. Isogeometric shell analysis with kirchhoff–love elements. *Computer methods in applied mechanics and engineering*, vol. 198, n. 49-52, pp. 3902–3914, 2009.

[3] T.-K. Uhm and S.-K. Youn. T-spline finite element method for the analysis of shell structures. *International Journal for Numerical Methods in Engineering*, vol. 80, n. 4, pp. 507–536, 2009.

[4] W. Dornisch, S. Klinkel, and B. Simeon. Isogeometric reissner–mindlin shell analysis with exactly calculated director vectors. *Computer Methods in Applied Mechanics and Engineering*, vol. 253, pp. 491–504, 2013.

[5] P. Hao, X. Yuan, C. Liu, B. Wang, H. Liu, G. Li, and F. Niu. An integrated framework of exact modeling, isogeometric analysis and optimization for variable-stiffness composite panels. *Computer Methods in Applied Mechanics and Engineering*, vol. 339, pp. 205–238, 2018.

[6] K. Bathe. *Finite Element Procedures in Engineering Analysis*. Prentice-Hall civil engineering and engineering mechanics series. Prentice-Hall, 1982.

[7] R. D. Cook and others. *Concepts and applications of finite element analysis*. John wiley & sons, 2007.

[8] M. Crisfield. *Non-linear Finite Element Analysis of Solids and Structures: Essentials*. Non-linear Finite Element Analysis of Solids and Structures. Wiley, 1991.

[9] A. Chajes. *Principles of Structural Stability Theory*. Prentice-Hall International Series in Management. Prentice-Hall, 1974.

[10] K. Sze, X. Liu, and S. Lo. Popular benchmark problems for geometric nonlinear analysis of shells. *Finite elements in analysis and design*, vol. 40, n. 11, pp. 1551–1569, 2004.